CHAPTER 1

INTRODUCTION

1.1 HISTORICAL PERSPECTIVE OF SILICON NANOWIRES

One-dimensional silicon (Si) wire was first discovered as (111) oriented Si whisker reported by Treuting and Arnold in the 1950s (*Treuting and Arnold 1957*). A later work on Si whisker grown on gold (Au) coated Si substrate by chemical vapour deposition (CVD) using tetrachlorosilane ($SiCl_4$) vapour decomposed at temperature of 800^oC was reported by Wagner and Ellis in 1964 (*Wagner and Ellis 1964*). They proposed a vapour-liquid-solid (VLS) growth mechanism for this metal-catalyzed epitaxial Si wire. This work was followed up by Givargizov (*Givargizov 1975*) using the same technique, while the kinetic for VLS mechanism was further developed with the experimental observations. Prior to this, the term Si whisker was commonly used rather than Si wire to describe this one-dimensional structure. The term silicon nanowires (SiNWs) was first used in the middle of the 90s (*Westwater et al. 1997*).

However, research on SiNWs remained inactive until it was stimulated in the late 90s when the study on one-dimensional carbon nanotubes became the focus of interest of researchers. It was discovered then that SiNWs showed semiconducting properties compatible to carbon nanotubes. This led to the increasing interest in experimental works exploring the formation of SiNWs using various techniques. Growth of SiNWs using laser ablation (*Morales and Lieber 1998*), thermal evaporation *(Wang et al. 1998*) and molecular beam epitaxy (*Liu et al. 1998*) techniques were first used in 1998, while, solution-based growth of SiNWs was demonstrated by Holmes et al. (*Holmes et al. 2000*) in 2000. The NWs were grown using diphenylsilane, $SiH_2(C_6H_5)_2$, solution mixed with

hexane and Au nanoparticles in a high pressure reactor.

In addition to the growth, another approach of top-down etching techniques also underwent significant development in large area fabrication of SiNWs. Electroless etching technique was first introduced by Peng et al. (*Peng et al. 2002*), and it is becoming one of the recent actively investigated techniques inspired mainly by its simple handling and low production cost. Wafer scale production of tip-like SiNWs fabricated by dry etching technique using electron-cyclotron resonance (ECR) plasma process was developed later by Chen et al. (*Hsu et al. 2004*).

The more recent successful attempt to utilize radio frequency plasma enhanced CVD (rf-PECVD) (*Zeng et al. 2003*), microwave plasma CVD (*Sharma and Sunkara 2004*), electron-cyclotron resonance (ECR)-CVD (*Cervera et al. 2010*) and hot-wire CVD (HWCVD) (*Govindarajan et al. 2009*) in synthesis of SiNWs has offered an opportunity for low temperature (< 500^{o}C) growth of NWs using CVD. This appears to be more practical than conventional CVD growth to meet industry needs.

1.2 MOTIVATIONS AND OBJECTIVES

The recognition of the novel potential of SiNWs for applications as nanosensors (*Hahm and Lieber 2004*), NW-based solar cells (*Garnett and Yang 2008; Perraud et al. 2009*), thermoelectric devices (*Boukai et al. 2008; Hochbaum et al. 2008*), tunable light emitters (*Chern et al. 2010; Walavalkar et al. 2010*), and anodes in lithium-ion batteries (*Chan et al. 2008; Laïk et al. 2008; Liu et al. 2011*) has created great interest among researchers. Considering that the amorphous Si technologies took more than 60 years to mature and emerge in a variety of electronic applications, SiNW technology is still in its infancy stage for current technological applications. One of the main reasons is the high cost of

large-scale industrial production. Low temperature and a large area synthesis of well-aligned SiNWs are the main requirements to satisfy current industrial, scientific and technological applications of SiNWs. CVD via VLS growth remains one of the most promising techniques in the large area synthesis of highly crystalline SiNWs. In the VLS growth process, the catalyst plays a key role in initiating the nucleation and growth of the NWs. Investigations have shown that the diameter of the NWs can be controlled by controlling the size of the catalyst (*Cui et al. 2001; Wu et al. 2004*); while selective area growth (*Sekhar et al. 2006*), self-assembly (*Englander et al. 2007; Sharma et al. 2005b*) and good alignment of NWs (*Dzbanovsky et al. 2005; Englander et al. 2007*) could be achieved by manipulating the parameters of catalyst formation. To date, knowledge regarding the VLS mechanism, from nucleation to growth (*Givargizov 1975; Kim et al. 2008; Wu and Yang 2001*), catalyst kinetics (*Hannon et al. 2006; Kodambaka et al. 2006; Madras et al. 2010*), and termination of growth (*Kolasinski 2006*) of SiNWs are well-documented.

Conventional CVD growth of SiNWs is limited by its high processing temperature. Average temperatures of ~600 and ~800^{o}C are required to initiate the growth of NWs by dissociating the source gases of silane (SiH_4) (*Sharma et al. 2005a*) and $SiCl_4$ (*Hochbaum et al. 2005*), respectively. In order to effectively reduce the growth temperature, two fundamental aspects need to be considered, namely the melting/eutectic point of the catalyst and the operating temperature of the CVD processing. Low melting point metals, such as gallium (30^{o}C), indium (157^{o}C), and stannum (232^{o}C), are currently preferred over Au (eutectic point ~370^{o}C) to obtain low temperature growth of SiNWs. These metal catalysts are classified as low Si solubility metal catalysts, which form eutectic composition with Si at concentrations of almost zero (smaller than 0.01 atom %) (*Schmidt et al. 2010*). Additionally, their low Si solubility can prevent the diffusion of

catalyst into NWs matrix, thus increases the purity of the SiNWs (*Zardo et al. 2010*). It is worth to mention that Au is well known to contaminate SiNWs which causes deep traps in the Si bandgap (*Iacopi et al. 2007*). Growth of SiNWs from indium (In) is possible at much higher precursor pressure in order to initiate nucleation for NWs formation. On the other hand, low temperature CVD, such as PECVD (*Bettge et al. 2009; Iacopi et al. 2007; Sharma and Sunkara 2004; Zardo et al. 2010*), pulsed PECVD (*Parlevliet and Cornish 2006*), microwave CVD (*Dzbanovsky et al. 2005; Sharma and Sunkara 2004*), ECR-CVD (*Cervera et al. 2010*) and HWCVD (*Govindarajan et al. 2009; Meshram et al. 2011*) have been introduced for the synthesis of SiNWs to effectively enhance the SiH_4 dissociation rate in CVD process. The formation of good quality SiNWs at substrate temperature below 400^{o}C has been achieved by several groups (*Hofmann et al. 2003; Yu et al. 2009*) with carefully chosen catalyst and system parameter settings.

The main objective of this work is to synthesize good quality (less defect and high crystallinity), high density and well aligned SiNWs at low temperature using a home-built dual mode plasma-assisted hot- wire chemical vapour deposition system. The study on the influence of the growth parameters, technique and catalyst used in the growth and structural properties of the SiNWs is another focus of this work. In order to achieve this objective, the following different processes of SiNWs growth are studied:

1. Formation of SiNWs using Au catalyst on hydrogen (H_2) plasma treated p-type c-Si(111) and indium tin oxide (ITO) coated glass substrates: The morphology and structural properties of the NWs formed on these two substrates are investigated and compared.
2. Formation of SiNWs using Au catalyst by simultaneous evaporation of Au wire using hot filament and dissociation of SiH_4 in H_2 plasma environment on ITO coated glass substrate: The morphology and structural properties of the NWs

formed with respect to the rf power applied are studied.

3. Formation of SiNWs by the HWCVD technique using In catalyst: Evaporation of In wire in H_2 plasma precedes the dissociation of SiH_4 diluted in H_2. The effect of In catalyst size on the formation, morphology and structural properties of the NWs is studied.
4. Formation of SiNWs by the HWCVD technique using In catalyst: Evaporation of In wire in H_2 plasma precedes the dissociation of SiH_4 diluted in H_2. The effects of filament temperature and deposition time on the formation, morphology and structural properties of the NWs are investigated.

1.3 OVERVIEW OF THESIS

The thesis is written in six chapters; literature review on the progress of SiNWs studies (Chapter 2), preparation of SiNWs (Chapter 3), results of each characterization on the SiNWs accompanied by discussion (Chapters 4 and 5), and wind up with conclusion and suggestions for future works (Chapter 6).

In Chapter 2, the more recent developments on the fundamental and applications of SiNWs are discussed. Two approaches for the SiNWs formation, namely top-down and bottom-up are described in brief, while the bottom-up approach of VLS growth process is emphasized. Metal-catalyzed CVD is well-known as one of the most promising techniques in VLS growth of SiNWs. The SiNWs grown by thermal CVD, PECVD and HWCVD will be described. In order to construct a basic understanding of the deposition process, setup of the reactor, elementary SiH_4 decomposition process and vapour phase reactions involved in the thermal CVD, PECVD and HWCVD are also discussed. The chapter ends with a review of several reports of SiNWs works on their novel structures, complemented by the growth mechanisms.

Details about setup of the home-built dual mode plasma assisted hot-wire CVD system and operating procedures of the system for SiNWs deposition are demonstrated in Chapter 3. In section 3.1, six important parts in the plasma and hot-wire assisted CVD system, covering the CVD reactor, plasma generator, hot-wire power supply, vacuum system, gas management, and heating elements are described. Substrates and source of metal catalyst used in this work are mentioned in Section 3.2. Details of the deposition procedures for five sets of SiNWs samples prepared in this work are presented in Section 3.3. In the following section, the analytical techniques employed to characterize morphology, chemical composition and structural properties of the samples are explained as well.

Chapters 4 and 5 discuss results of the characterization on the as-grown SiNWs samples. In chapter 4, growth of SiNWs using Au catalyst and PECVD technique is studied by in situ evaporation of Au wire to form catalyst islands and plasma decomposition of SiH_4 and H_2 gases to form SiNWs. The catalyst islands and NWs formations on c-Si and ITO coated glass substrates are investigated and compared. This is followed by the study on the growth of SiNWs by simultaneous Au evaporation and SiH_4 and H_2 gases decomposition using hot-wire assisted PECVD technique on ITO coated glass, while, the effect of rf power on the morphology and structural properties of the SiNWs is investigated. Thereby, the mechanisms of the catalytic growth of SiNWs using Au evaporation followed by SiNWs deposition on c-Si and ITO coated glass, and simultaneous Au and SiNWs deposition on ITO coated glass are proposed. Chapter 5 discusses study of the In-catalyzed SiNWs using HWCVD technique. The deposition is carried out by in-situ evaporation of In wires in a H_2 plasma environment, followed by SiH_4 and H_2 gases decomposition using HWCVD. The effects of In catalyst size, filament

temperature and deposition time on the growth and structural properties of the In-catalyzed SiNWs are systematically investigated. These works are completed by the growth models of the In-catalyzed HWCVD grown SiNWs at the end of the chapter.

Finally, conclusion and suggestions for future work are presented in Chapter 6. The results and discussion in Chapters 4 and 5 aid to build up the conclusive ideas on the formation of well-aligned and highly crystalline SiNWs at low temperature by employing In instead of Au as catalyst and replacing plasma with HWCVD as deposition technique. The potential applications of these SiNWs such as field emitter, NWs based solar cell and thermoelectric device are suggested for future research.

CHAPTER 2

LITERATURE REVIEW

2.1 NANOTECHNOLOGY AND NANOMATERIALS

Nanotechnology is known as the fabrication, design and application of nanostructures and nanomaterials. It involves study of the fundamental physical properties and phenomena of nanostructures and nanomaterials (nanoscience) and covers the processing of their applications (*Cao 2004*). Typical sizes of the nanostructures range from several to several hundred nanometers (10^9 – 10^7 m). The dimensions of the nanostructures extend from zero dimensional (nanoparticle and quantum dot) to one dimensional (nanowire and nanotube), and two dimensional thin film structures. Examples of nanomaterials which have generated a huge amount of research include metal nanoparticles, SiNWs, carbon nanotubes, metal oxide nanorods and graphene. The interest in nanomaterials is mainly because they exhibit structural, optical and electrical properties which are distinctively different from their bulk or even micron-scaled of the materials. For example, Au nanoparticles reveal surface plasmon resonance (*Eustis et al. 2006*) and Si quantum dots emit visible light (*Kim 1998*), which are totally absent in their bulk materials. Thus, the study on nanomaterials is always aimed at discovering their unique properties and behaviors to build up the fundamental understanding of these materials. The research on these nanomaterials is further developed to design and integrate them into devices to merge the nanomaterials into nanotechnology development.

2.1.1 Realization of the importance of Si nanowires

Nanowires refer to one-dimensional wire, rod, tip, whisker and cone-like structures with diameter of less than 100 nm. NWs have stimulated tremendous research interest due to

their small dimension and unique properties which allow them to be integrated into nanoelectronics, nanophotonics and nanodevices applications (*Wan et al. 2009b; Yan et al. 2009*).

2.1.1 a) Significant increase in works on nanowires

The significant increase in the number of publications on NWs-related topics in the last ten years (Figure 2.1) indicates that the field of NWs has become one of the most actively research in the field of nanotechnology. These research papers cover fundamental growth, physical characteristics, applications and models of metallic, semiconducting, insulating and heterostructured NWs. Among of these, SiNWs serve as the fundamental material in the field of semiconducting NWs. Although the research on SiNWs has begun in the 90's, it is still remaining a very popular subject among researchers. One of the reasons is because SiNWs can be easily incorporated into the current matured Si-based device technology. Theoretical prediction shows their semiconducting as well as electrical properties are not influenced by the nanoscaled structures (*Rurali 2010*).

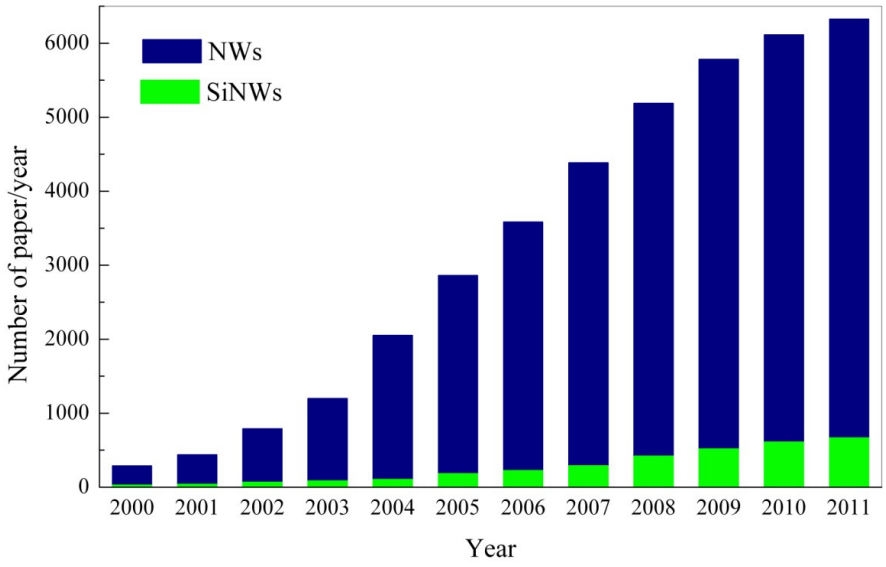

Figure 2.1: Number of publications on NWs and SiNWs-related topics from year 2000-2011. (Source: ISI, keywords: nanowires and silicon nanowires)

2.1.1 b) Novel physical properties and phenomena of Si nanowires

SiNWs reveal very different optical, surface tension and thermal properties compared to the bulk Si (*Bandaru et al. 2010; Kazan et al. 2010*). One of the great examples is the enhancement of optical absorption of SiNW arrays. Figure 2.2 (a) shows photographs of a 4-inch bulk Si wafer (right) and a Si wafer coated with 10 μm length of SiNW arrays (left). It is clearly seen that surface of the Si wafer becomes non-reflecting when coated with SiNW arrays. The sub-wavelength diameters of SiNW arrays are able to trap the photon and enhance the photon absorption due to their significant higher surface area to volume ratio than the bulk Si wafer. As a result of this, the optical absorption ability is much improved over a wide range of wavelengths and angles with the SiNWs coatings.

SiNWs show various colours over the full range of visible spectrum, which is distinctively different from the grey colour of the bulk Si (*Cao et al. 2010*). Seo et al (*Seo et al. 2011*) show that each NWs exhibits their own individual colour, while the colours are dependent on the diameters of the NWs. Figure 2.2 (b) and (c) show the optical image under bright-field illumination and the SEM image of the patterned vertical SiNW arrays, respectively. The SiNWs with diameters of 45, 50 and 65 nm are represented by the red, blue and green colours in the optical image, respectively.

Further scaling down the diameter of SiNWs to quantum size of < 10 nm can result in a transformation of Si from indirect to direct bandgap material due to quantum confinement effect. This allows the photoluminescence (PL) and electroluminescence from the Si quantum wires. Tunable visible to near infrared PL emission from sub-10 nm Si nanopillars is reported by several groups (*Guichard et al. 2006; Walavalkar et al. 2010*). A blue shift in PL energy with narrowing of the pillar diameter is generally observed. This shows that wide range of PL can be obtained by precisely controlling the

diameter of Si nanopillars within 10 nm.

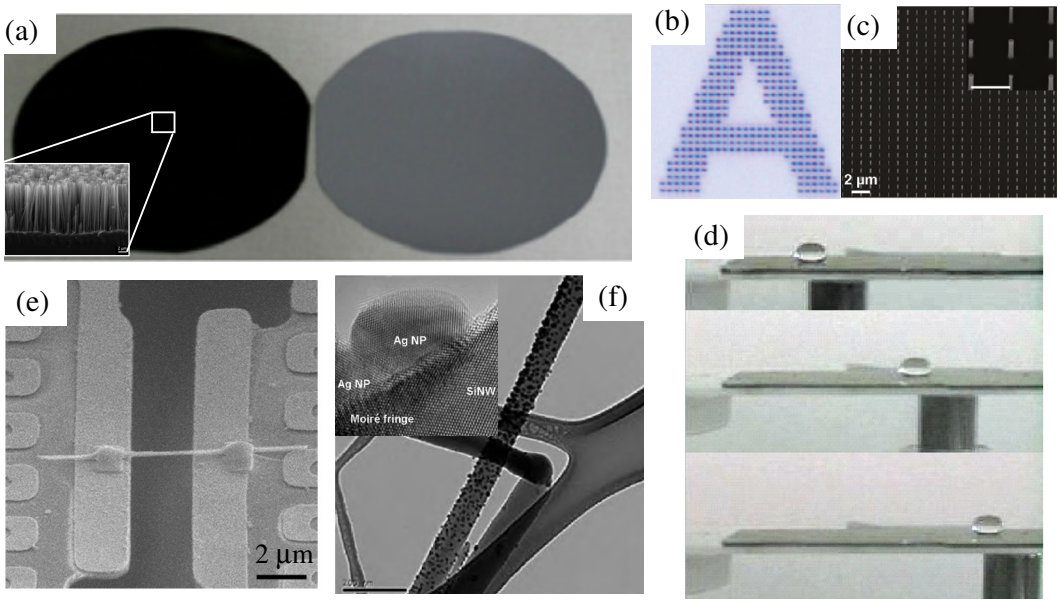

Figure 2.2: (a) Photographs of a 4-inch Si wafer (right) and coated with 10 µm of SiNWs (left). The inset shows the SEM image of the electroless metal deposited SiNW arrays (*Ozdemir et al. 2011*). (b) Bright-field optical microscope image of patterned vertical SiNW arrays, and (c) a 30 ^{o} tilted SEM image of Bayer filter pattern which consists of vertical SiNWs with radii of 45, 50 and 65 nm, representing red, blue and green colours, respectively. Inset in (c) is magnified SEM image (*Seo et al. 2011*). (d) SEM image of a platinum-bonded SiNWs taken at 52 ^{o} tilt angle (*Hochbaum et al. 2008*). (e) TEM image of silver nanoparticles modified SiNWs. Inset in (e) is HRTEM image of silver nanoparticles embedded in the surface of SiNWs (*He et al. 2010*). (f) Sequence of frames from a video of a 30 ml water drop moving from left to right on a SiNW superhydrophobic surface with iron particles (concentration of 5%) by the action of a permanent magnet below the surface (*Egatz-Gómez et al. 2007*).

Structuring the bulk Si to uniform arrays of SiNW can also bring new phenomenon such as superhydrophobicity. SiNW arrays exhibit much lower surface energy due to its micro/nanoscaled surface roughness. The low surface energy significantly increases the water contact angle, resulting in the superhydrophobic surface (also known as 'lotus effect'). The high mobility of water without splitting on the surface of a SiNW arrays [Figure 2.2 (d)] proves their potential for fog condensation, anti-water coalescence and self-cleaning coating applications (*Egatz-Gómez et al. 2007*).

The one-dimensional structure of NWs can be abstracted from the growth substrate to make single NWs devices [Figure 2.2 (e)]. This makes them useful as basic building

blocks of nanoelectronics, such as NWs field effect transistor (FET) (*Cui et al. 2003; Schmidt et al. 2006*), nanosensors (*Patolsky and Lieber 2005*), polarization-sensitive detectors (*Ahn et al. 2005*) and biological pore transportation channels (*Martinez et al. 2009*). The surface of the SiNWs can be modified by decorating it with metal nanoparticles to enhance their sensing ability (*He et al. 2010*) and surface enhanced Raman scattering (*Zhang et al. 2010*).

2.1.1 c) Wide range of potential applications

The unique physical properties and phenomena of SiNWs have attracted considerable interest in development of near future nanodevices applications. Implementation of SiNWs in several promising fields of applications such as SiNWs-FET, photovoltaic devices, Lithium-ion battery and thermoelectric devices are briefly discussed.

The large surface to volume ratio and high sensitivity of the SiNWs-FETs are applicable in nanoscale of pH sensor (*Chen et al. 2006*), gas sensor (*Wan et al. 2009a*) and biological sensor (*Zhang et al. 2009*). The sensing mechanism of SiNW is generally due to the change of its electrical conductance upon the direct binding of electron withdrawing species or electron donating species onto the Si surface or exposure to charged biological molecules surrounding it. The detection limit of femtomolar concentration can be achieved by SiNWs sensor, which shows high sensitivity of NWs due to its large surface structures.

High photon absorption properties of SiNWs are suited for the solar cell and photovoltaic devices. To construct SiNWs solar cell, the SiNWs are doped (in-situ or ex-situ) to form p-i-n coaxial SiNWs. Each individual NW can ideally act as an individual solar cell. The single coaxial SiNW p-i-n junction solar cell demonstrated by

Tian et al (*Tian et al. 2007*) shows efficiency up to 3.4%, while SiNW arrays solar cells with efficiency > 10% have been demonstrated by several groups (*Fang et al. 2008; Huang et al. 2012; Xu et al. 2011*). The performance of SiNWs solar cells can be improved by surface passivation of SiNWs to limit the interfacial recombination (*Garnett and Yang 2008*).

SiNWs anodes reveal better performance compared to the existing graphite anodes in lithium-ion battery. SiNWs anodes have higher theoretical specific capacity of 4200 $mAhg^{-1}$ than graphite (372 $mAhg^{-1}$) (*Chan et al. 2008*), longer life cycle and better resistance to pulverization during cycling. Some reported works (*Maranchi et al. 2003; Yin et al. 2006*) suggested that amorphous Si anodes have better cycling performance compared to the crystalline Si due to the lower volume expansion and higher potential of amorphous Si when reacting with Li^+ ions. Cui et al. (*Cui et al. 2009*) reported an improvement in the life cycle of lithium-ion battery to more than 100 cycles when crystalline-amorphous core-shell SiNWs anodes are used.

Yang et al (*Hochbaum et al. 2008*) and Heath et al. (*Boukai et al. 2008*) are among the first to report on the high thermoelectric conversion efficiency of SiNWs (as much as 100 times of bulk Si), making it a good candidate for thermoelectric device application. The thermal conductivity of SiNW is significantly reduced to ~1.6 $Wm^{-1}K^{-1}$ compared to bulk Si (~150 $Wm^{-1}K^{-1}$), while the electrical conductivity remains bulk-like. The thermal conductivity of SiNWs could be further reduced by introducing defects in the structure (*Hochbaum et al. 2008*) and reducing the NW diameters (down to 10 nm) (*Boukai et al. 2008; Shi et al. 2009*) to reduce phonon transport.

From the view point of the increasing number of publications, the novel physical

properties and wide range of potential applications of SiNWs, the role of SiNWs in future technology is indubitable. The applications as mentioned above are much dependent on the construction and surface passivation of SiNWs. Large-scale and low cost (low energy consumption) production of high quality SiNWs is an important issue to be considered by researchers.

2.2 DEVELOPMENT ON THE FABRICATION AND SYNTHESIS OF SILICON NANOWIRES

Since the discovery of one-dimensional SiNWs, much effort has been made to construct these nanostructures. It is well known that top-down and bottom-up methods are two approaches widely used in the fabrication/synthesis of SiNWs. The schematic of the top-down and bottom-up approaches in the formation of SiNWs is shown in Figure 2.3. Numerous deposition techniques have been introduced and developed in the preparation of SiNWs based on these two approaches.

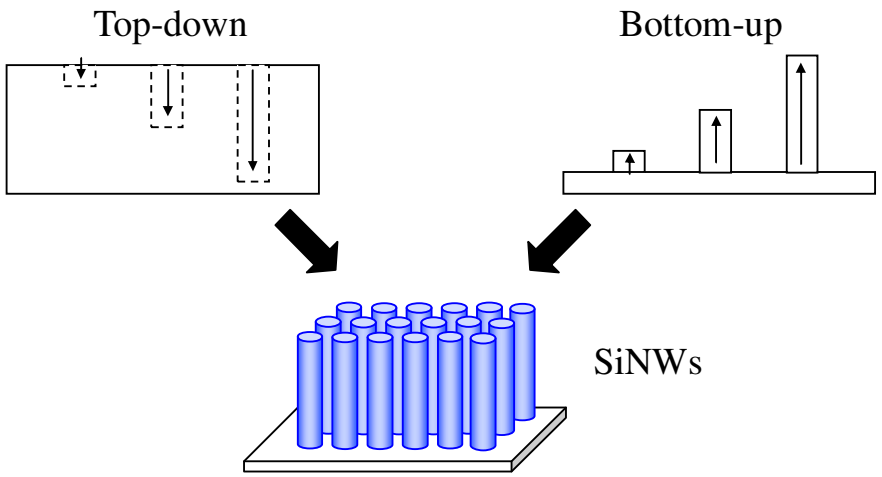

Figure 2.3: Top-down and bottom-up approaches in the formation of SiNWs.

2.2.1 Top-down method

The top-down method for SiNWs formation is generally done by etching of pre-formed Si layer or Si substrate to form one-dimensional structures. It can be done by using

either dry or wet chemical etching process. Dry etching refers to the electron-beam lithography, reactive ion bombardment and plasma etching. These techniques usually require complex and high cost optical equipment and complicated handling process. Alternatively, chemical etching which is performed by using liquid etchants is comparatively cheap and easy to use. Hydrofluoric acid (HF) solution is usually used for silicon dioxide (SiO_2) etching. One good example is the electroless etching of silver (Ag)-treated Si substrate in HF/$Fe(NO_3)_3$ solution (*Peng et al. 2006*). The oxidation of Si occurs by reducing the Fe^{3+} to Fe^{2+} resulting in the formation of SiO_2 surrounding the Ag. The SiO_2 is then etched away by HF. The etching process is continued to form vertical SiNW arrays. The top-down methods are advanced for the fabrication of high uniformity and vertical aligned SiNW arrays. However, they still face some limitations such as structure defects, imperfection of the surface and impurities. For example, surface crystallography damage is observed for electroless etching fabricated SiNWs (*Hochbaum et al. 2008*), while, Si nanotips fabricated using ECR plasma etching have silicon carbide (SiC) impurities on the surface of the nanotips (*Hsu et al. 2004*).

2.2.2 Bottom-up method

Bottom-up method refers to the building up of a material atom-by-atom from the bottom. The process involves a one-dimensional growth evolving from Si containing sources. Laser ablation, thermal evaporation, solution-based growth, CVD, MBE and magnetron sputtering generally obey the bottom-up growth method. The difference between these techniques is mainly associated with the difference in the Si source supplied for the growth. Laser ablation utilizes a solid target of mixed Si-Fe elements for the growth (*Morales and Lieber 1998*). Solution-based growth is performed using solution of monophenylsilane ($SiH_2C_6H_8$) or $SiH_2(C_6H_5)_2$ as precursor to yield the one-dimensional growth (*Holmes et al. 2000*). CVD grown SiNWs employs Si-containing vapour such as

$SiCl_4$ or SiH_4 gases as the source (*Sharma et al. 2005a; Hochbaum et al. 2005*),. The growth mechanisms of the SiNWs by these techniques include VLS (*Kolasinski 2006*), vapour-solid-solid (*Wang et al. 2006*), solid-liquid-solid (*Wong et al. 2005*), solution-liquid-solid (*Heitsch et al. 2008*), oxide-assisted growth (*Lee et al. 2000*), sulfide-assisted growth (*Niu and Wang 2008*) and template-based growth (*Huang et al. 2008*). By far, VLS is the most wide- adopted mechanism.

The bottom-up growth technique is able to produce less structured defects and good crystalline quality of SiNWs by controlling the deposition parameters (*Cao 2004*). For example, monocrystalline SiNWs can be induced by metal catalysts due to their perfect crystalline structures, while, epitaxial growth of SiNWs on c-Si substrate is possible provided the substrate is well treated to get rid of the native oxide layer. A direct in situ doping of the NWs can be carried out together with the growth of SiNWs in the gas phase using CVD (*Garnett et al. 2009; Perea et al. 2009*). Another important advantage of the bottom-up method is the ability to grow smaller diameters of SiNWs. The thinnest SiNWs with diameter of 1.3 nm is obtained by oxide-assisted growth via thermal evaporation of SiO_2 powder (*Ma et al. 2003*). However, the preferred orientation of the bottom-up grown SiNWs is dependent on the diameter of the NWs, regardless of the synthesis techniques.

2.3 VAPOUR-LIQUID-SOLID GROWTH MECHANISM

VLS growth model of one-dimensional structures was first introduced by Wagner (*Wagner and Levitt 1970*) and further modified by Givargizov (*Givargizov 1987*). Their proposed model has been widely applied in catalytic one-dimensional growth of a variety of materials. Today, the VLS growth model has gone through various developments owing to the excellent research in this area.

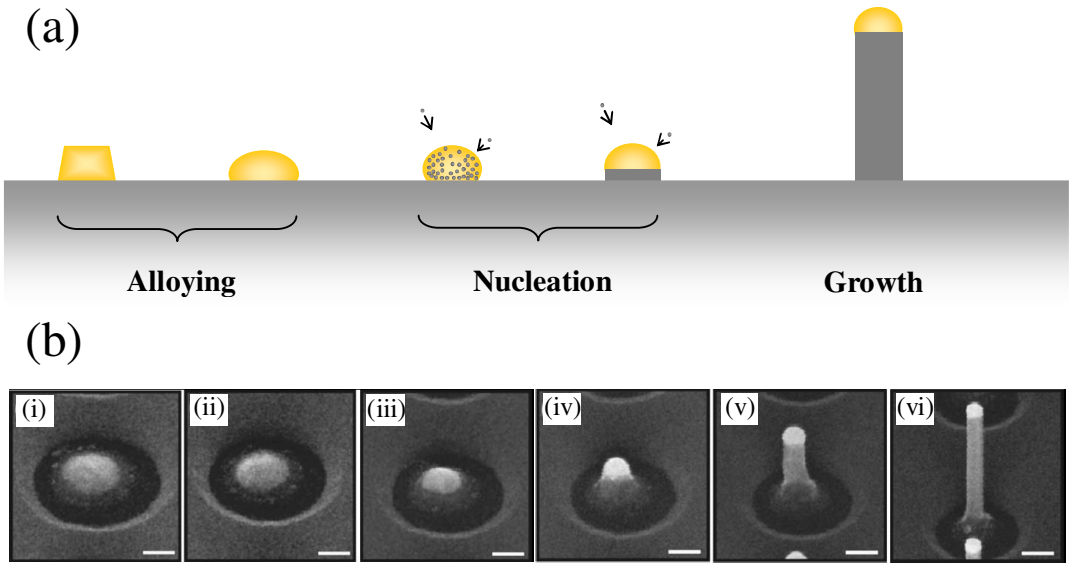

Figure 2.4: (a) VLS growth mechanism of SiNWs. (b) FESEM micrographs of the growth process of Au-catalyzed SiNWs (scale bar = 100 nm) (*Schmid et al. 2008*).

2.3.1 VLS growth model

In VLS mechanism, a metal catalyst is employed to initiate and direct the growth of SiNWs. In general, the growth process can be divided into three parts, namely alloying, nucleation, and growth [Figure 2.4 (a)]. The catalyst forms liquid by itself or alloys with Si on a substrate. The Si precursors tend to diffuse into the catalyst due to the catalytic action of the metal catalyst. The beginning of the Si diffusion into the catalyst takes a period for nucleation process. Continuous diffusion of Si into the liquid catalyst leads to saturation and subsequently forms precipitation on the liquid-solid interface. This results in the one-dimensional growth of SiNWs. Figure 2.4 (b) demonstrates the investigation on VLS growth process of Au-catalyzed SiNWs using SEM, reported by Schmid et al. (*Schmid et al. 2008*). The evolution of a flat Au film into Au droplet on top of the NWs as well as the nucleation and steady growth of SiNWs are clearly shown in Figure 2.4 (b) i – vi. In order to have a better understanding of the VLS mechanism, each process of growth is presented separately in the following section.

2.3.2 Catalyst

In VLS growth process, a molten metal catalyst plays a very important role, acting as a medium for the deposition of Si precursors. Several criteria must be fulfilled by a metal catalyst in order to initiate the growth (*Cao 2004*). The catalyst must be inert to any chemical reaction with the Si precursors. The distribution coefficient of the catalyst must be less than unity at the deposition temperature, so that it will remain as individual particle. The equilibrium vapour pressure of the catalyst over the liquid droplet must be very small to maintain steady growth of SiNWs. The wetting characteristic of the catalyst and the substrate will influence the diameter of the grown nanowire. Under the same particle size, low wettability catalyst tends to form smaller size NWs than high wettability catalyst.

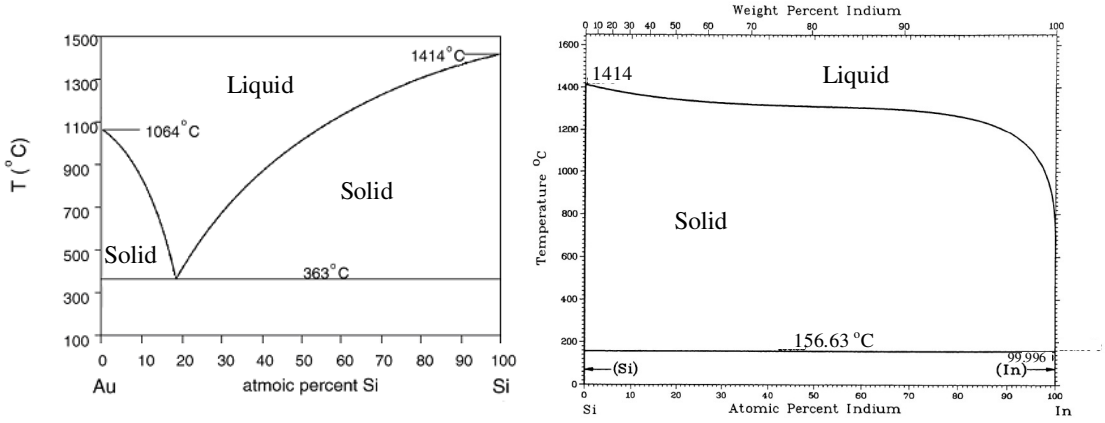

Figure 2.5: Phase diagram of (a) Au-Si (*Anantatmula et al. 1975*), and (b) In-Si system (*Olesinski et al. 1985*).

Au is the most commonly used catalyst to induce the growth of SiNWs. The advantages of Au are its high chemical stability, resistance to oxidization, and strong catalytic ability (*Schmidt et al. 2010*). Au forms an alloy with Si which has a low eutectic point of 363^{o}C at a composition of 18.6% Si [Figure 2.5 (a)]. It can induce the growth of SiNWs at temperatures lower than 400^{o}C. However, Au is associated with deep-level defects in SiNWs, and this is incompatible with the metal-oxide-semiconductor and Si

industry. Furthermore, Au is well known to contaminate the surface of the NWs due to migration and diffusion of the catalyst (*Kawashima et al. 2007; Madras et al. 2010; Xu et al. 2010*). Thus, a large variety of materials, such as ferrum (Fe), nickel (Ni), platinum (Pt), palladium (Pd), copper (Cu), cobalt (Co), aluminum (Al), stannum (Sn), In, and gallium (Ga) have been tested as catalyst alternatives to the Au (*Nebol'sin and Shchetinin 2003; Schmidt et al. 2010; Yuan et al. 2011*).

Schmidt et al. (*Schmidt et al. 2010*) divide the metal catalyst into three categories according to their behaviours, namely, Au-like metals, silicide forming metals, and low Si solubility metals. Low Si solubility metals, such as Sn, In and Ga are currently favoured due to their low melting temperature. In is attractive from an electronics viewpoint as it can induce p-type doping in the SiNWs (*Schmidt et al. 2010*). In has a low melting point of 156.6^{o}C. Thus, lower temperature growth of SiNWs is expected to be achieved using In via VLS process. However, due to its low Si solubility (~1 x 10^{-15} cm^2/s), much higher Si precursor pressures are required to induce the growth. In particle is easily oxidized to form indium oxide (In_2O_3) on its surface, which might reduce its catalytic effect. Fortunately, the In_2O_3 can be reduced by H radicals via H_2 plasma treatment (*Alet et al. 2008*), while the oxidation of In particle can be minimized by combining the In evaporation and SiNWs growth in one deposition (*Convertino et al. 2011*).

2.3.3 Vapour source of Si

SiH_4, disilane (Si_2H_6), trisilane (Si_3H_8), $SiCl_4$ and dichlorosilane (SiH_2Cl_2) have been tested as Si precursors to produce SiNWs using CVD. The early work on SiNWs was carried out using $SiCl_4$ (*Givargizov 1975; Wagner and Ellis 1964*) However, typical higher temperature (> 800^{o}C) is required to thermally decompose $SiCl_4$, (*Garnett et al.*

2007; Krylyuk et al. 2011) while, dilution of H_2 in the $SiCl_4$ tends to create hydrochloric acid, which can cause etching effect on the sample (*Schmidt et al. 2006; Schmidt et al. 2010*). Thus, SiH_4 is becoming the favourite precursor due to its lower decomposition temperature and chlorine-free process. It is found that SiH_4 usually induces smaller size of SiNWs than $SiCl_4$ (*Westwater et al. 1997*). SiH_4 can be decomposed into SiH_2 species at temperature of ~400^{o}C. The SiH_2 species will then completely decompose into Si atoms at the surface of the liquid catalyst, resulting in a steady supply of Si element into the catalyst. The transport of Si atoms from the catalyst surface into the interface of the catalyst and substrate must be fast enough to avoid the depositing of the Si atoms on the catalyst surface and shield the growth of SiNWs. Utilization of plasma enhancement or hot-wire catalytic techniques in CVD can effectively crack the SiH_4 into more reactive species instead of thermally decomposing the precursors. Consequently, a large amount of SiH_x growth species/radicals can be generated. Thus, it allows the formation of SiNWs from low Si solubility catalyst using PECVD or HWCVD.

2.3.4 Nucleation

Saturation of the catalyst with the Si atoms may lead to an incubation time before the precipitation and growth. The process is called nucleation. It is the initial stage of NWs growth. In situ observation of the nucleation process using ultrahigh-vacuum transmission electron microscopy is demonstrated by Hofmann et al. (*Hofmann et al. 2008*) and Kim et al. (*Kim et al. 2008*). Figure 2.6 (a) shows bright field TEM images of a growing Si nucleus acquired at t = 102, 105 and 131 s, respectively. The elongation of Si nucleus from the Au catalyst can be clearly seen. Quantitative measurement of the variation of linear dimension of the Si nuclei with time was also presented by them (*Kim et al. 2008*) [Figure 2.6 (b)]. The catalyst took a certain time to elapse after the introduction of Si-containing precursors (defined as nucleation time). After reaching a

critical point for the growth, the Si nuclei start to grow very rapidly. The growth is slowed down after the steady growth stage is reached. Another important argument proved by them is the larger radius of catalyst droplets show a longer nucleation time. Kalache et al. (*Kalache et al. 2006*) studied the nucleation in the growth of SiNWs via Au- and Cu-catalytic VLS process. They showed that the nucleation time is inversely proportional to the growth temperature.

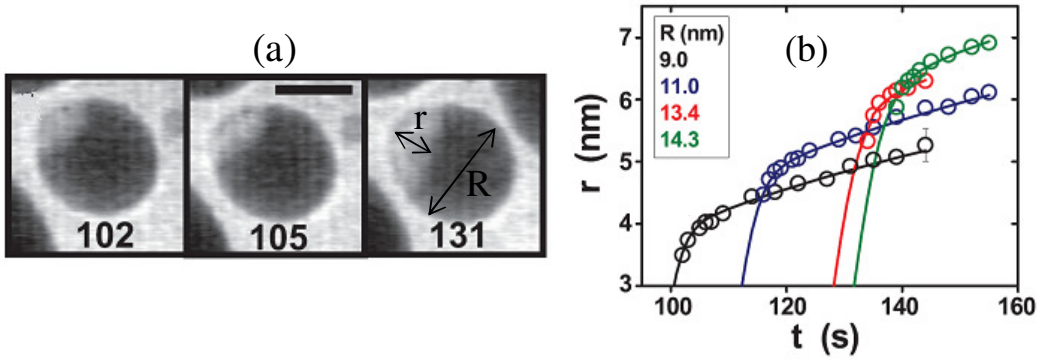

Figure 2.6: (a) Bright field TEM images of a growing Si nucleus acquired at time, *t* of 102, 105 and 131 s, respectively. (Scale bar = 10 nm). (b) Variation of linear dimension, r of Si nuclei with time for different radius of droplet, R (*Kim et al. 2008*).

2.3.5 Steady growth

Figure 2.7 shows the general considerations on the nucleation, steady growth and termination stages for the VLS growth SiNWs. The nucleation as well as the initial rapid growth of Si nuclei is discussed in the previous section. When the growth of Si nuclei reaches a constant rate ($dR_{axial}/dt = 0$), steady state of growth takes place. Once the steady state is reached, the continuous supply of the Si species into the catalyst will lead to the precipitation at the catalyst-nanowire interface. In this stage, the diameter of the catalyst is not evolving; therefore the grown NW remains uniform in diameter. Axial growth rate, R_{axial} of SiNWs is usually estimated by relation as (*Kikkawa et al. 2005*):

$$R_{axial} = \frac{l_{NW}}{t_d} \tag{2.1}$$

where l_{NW} is the length of the NW and t_d is the deposition time. However, a more

accurate calculation should include the nucleation time, t_{nuc}, provided the nucleation time of the catalyst is known. The relation can be written as (*Schmid et al. 2008*):

$$R_{axial} = \frac{l_{NW}}{t_d - t_{nuc}} \tag{2.2}$$

A variety of models regarding the growth rate of SiNWs has been developed to fit the experimental data by considering the pressure (SiH_4 partial pressure and total pressure) (*Wan et al. 2010*), temperature and pressure dependence (*Schmidt et al. 2010*) and NWs radius dependence (*Schmidt et al. 2009*).

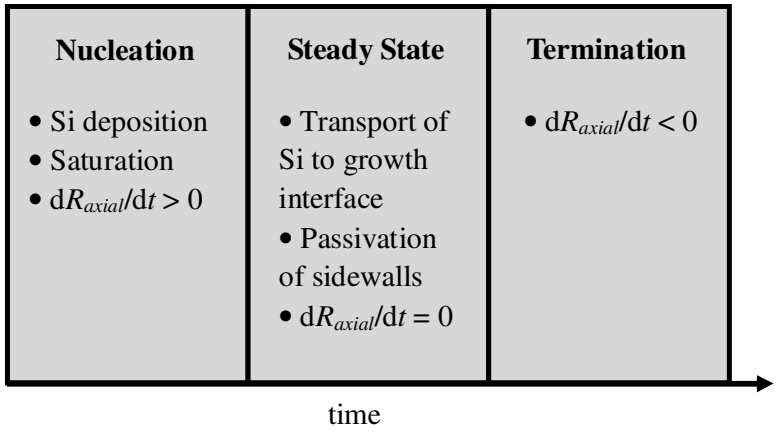

Figure 2.7: General considerations on the different stage that occur during the catalytic growth of SiNWs (*Kolasinski 2006*).

During the axial growth of SiNWs, reactive Si growth species can adsorb on the sidewalls of the NWs. This results in radial growth or sidewalls deposition. This process could increase diameter of the NWs or induce non-uniform diameter (tapering) NWs. The radial growth rate, R_{radial}, can be estimated from the radius of the NWs, r_{NW}, as:

$$R_{radial} = \frac{r_{NW} - r_O}{t_d} \tag{2.3}$$

where r_o is the initial radius of the NWs before the radial growth occurred. Schmidt et al. (*Schmid et al. 2008*) reported that the R_{radial} is ~2 orders of magnitude smaller than R_{axial}. Pressure and flow rate of Si precursor and carrier gases are important parameters contributing to the radial growth process. Krylyuk et al. (*Krylyuk et al. 2011*)

demonstrated the tapering control of SiNWs by controlling the pressure and total gas flow rate. They stated that the radial growth rate can be enhanced by reducing the deposition pressure, lowering the $SiCl_4/H_2$ molar ratio or applying a higher gas flow rate.

2.3.6 Termination of axial growth

The axial growth of SiNWs will be terminated if the temperature is reduced below a critical value or the catalyst is completely consumed (*Kolasinski 2006*). The temperature plays a crucial role in thermodynamic stability of the liquid phase of catalyst. Slight decrease in substrate temperature during the steady growth may reduce growth rate of the NWs (*Schmidt and Gösele 2007*). Thus, further decrease in substrate temperature to a critical point could lead to the termination of the growth. Another possible reason for the termination of growth is the evolution of the catalyst. During the NWs growth, the catalyst can be migrated through evaporation (*Cao et al. 2006; Hannon et al. 2006; Madras et al. 2010*) or incorporation into the NWs matrix (*Cao et al. 2006; Yu et al. 2011*). As a result, size of the catalyst could reduce and wind up with full migration of the catalyst. This is evident by the tapering on the top of the NWs; forming needle- or tip-like NWs. Vapour pressure is an important issue to prevent the migration of the catalyst.

2.4 GROWTH TECHNIQUES

2.4.1 Chemical vapour deposition

CVD is the oldest and one of the most promising techniques in the synthesis of SiNWs via catalytic VLS mechanism. CVD is also known as thermal CVD as it thermally decomposes source gas by heating. Thermal CVD can be categorized according to their working temperature, namely high temperature, moderate temperature and low temperature CVD. For high temperature CVD, the reactor is usually constructed by a quartz tube. Heating element is built outside, surrounding the quartz tube. One end of the tube supplies Si-containing vapour, the other end is connected to evacuation tools. The quartz tube reactor is heated up to a temperature of 700 – 1100^{o}C for the growth, thus it is also called hot-wall CVD. The substrate is placed within the hot zone (usually in the middle) of the tube. High temperature CVD is typically used for $SiCl_4$ precursor as it requires high temperature of > 800^{o}C for decomposition. However, the growth of SiNWs using $SiCl_4$ has slowed due to the yield of large diameter of NWs compared to SiH_4. Catalyst is also a criterion for the choice of high temperature CVD. For example, Ni and Fe catalyst require high temperature of ~1000^{o}C to reach eutectic point with Si, and producing NWs.

Moderate temperature CVD typically works at a temperature range from 400 to 700^{o}C. It is constructed by a stainless steel or quartz-made reactor, with heating element built inside the reactor. Different from high temperature CVD, only substrate rather than the reactor is heated up (cold wall). Hence, the decomposition of the precursor mostly occurs near the surface of the substrate. In moderate and low temperature CVD, SiH_4 is frequently used as precursor. In contrast to $SiCl_4$, SiH_4 already decomposes at temperature of ~400^{o}C. The SiH_4 molecules crack into silylene (SiH_2) species which need lower activation energy for the deposition. The decomposition process can be

written as:

SiH_4 (g) → SiH_2 (g) + H_2 (g) (2.4)

However, a higher temperature (~600^oC) is necessary for effective decomposition of SiH_4 gas. Thus, the better quality, less kinking and defects SiNWs are mostly synthesized at temperatures beyond 500^oC (*Madras et al. 2009*).

The main advantages of thermal CVD are the broader choice of catalyst and allowing epitaxial growth of SiNWs. The wide range of operating temperature of high temperature and moderate temperature CVD permits a large variety of metals to be involved in the growth. These metals include Au (*Givargizov 1975; Salem et al. 2009; Schmidt et al. 2005; Sharma et al. 2005a*), Ag (*Nebol'sin et al. 2005*), Al (*Wang et al. 2006*), Cu (*Arbiol et al. 2007; Kayes et al. 2007*), Ni (*Jee et al. 2010; Jin et al. 2001*), Fe (*Li et al. 2005; Liu et al. 2001*), Ti (*Sharma et al. 2004*), Pd (*Zhang et al. 2007*), Pt (*Jeong et al. 2009*), Au/Pd (*Liu et al. 2000*) and Ga/Au (*Lugstein et al. 2007*). Epitaxial growth of SiNWs on c-Si substrate is possible if the native oxide layer on c-Si substrate is eliminated prior to the catalyst formation. Epitaxial growth of <111> oriented SiNWs is reported by several groups using Al (*Wang et al. 2006*), Cu (*Kayes et al. 2007*) and Au (*Salem et al. 2009; Schmidt et al. 2005*), Ga/Au (*Lugstein et al. 2007*) as catalyst. Nevertheless, their temperature is relatively higher compared to the manufacturing temperature in industry (< 400^oC). Hence, the utilization of plasma and hot-wire in low temperature CVD is intended to enhance the decomposition process at low temperature.

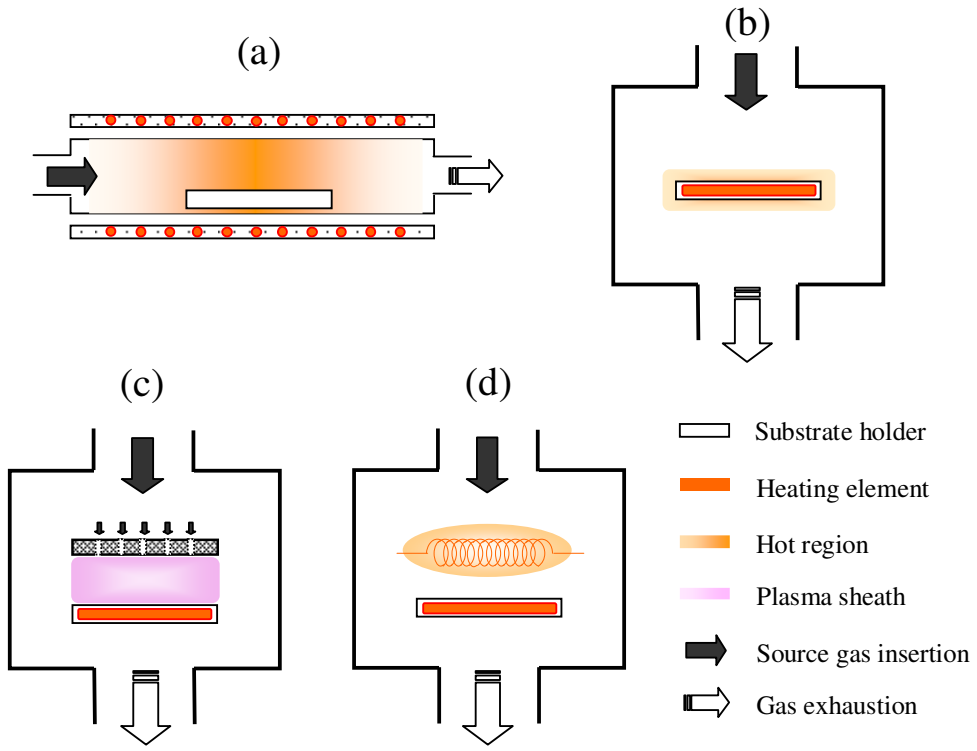

Figure 2.8: Simplified schematic diagrams of (a) high temperature CVD, (b) cold wall CVD, (c) PECVD, and (d) HWCVD reactors.

2.4.2 Plasma enhanced chemical vapour deposition

PECVD reactor consists of two electrodes made of stainless steel, which are placed in parallel at a distance of a few cm. The radio frequency (rf) generator is capacitively coupled to the top electrode, while the other electrode where the substrate is mounted is grounded. The powered top electrode is usually designed as showerhead, where the precursor and carrier gases can be focused into a plasma sheath through it.

Silane plasma is generated between the two electrodes at rf of 13.56 MHz (or higher). The plasma forms a sheath with the electrodes. This results in a potential difference (sheath voltage) across the sheath regions and electrodes. The plasma consists of electron, positive charged SiH_x and H ionic species, and neutral molecules of SiH_4. However, the plasma remains electrically neutral as the electron and positive ionic

species are balanced with each other. Electrons are decelerated by the sheath voltage, therefore being confined within the plasma, and leaving a low electron density in the sheath [Figure 2.9]. The electron density in the plasma is typically ~10^8 – 10^9 cm^{-3} for a pressure range from ~0.1 to hundreds mbar (*Surendra and Graves 1991a*). The kinetic energies of electron vary from several to tens of electron volts (eV), while kinetic energies of ionic species are about 50 – 100 MeV (*Surendra and Graves 1991b*).

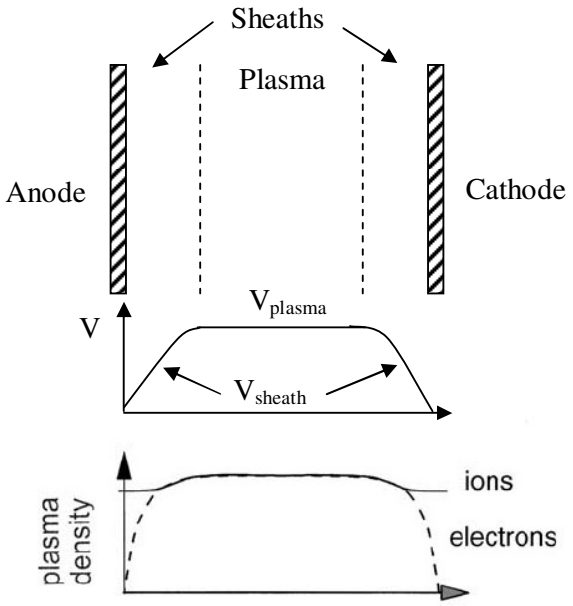

Figure 2.9: Potential difference and plasma (ions and electrons) density within plasma and sheath region.

The discharge of neutral molecules into ionic species is a spontaneous process. The dissociation of SiH_4 usually results in the formation of SiH_3, SiH_2, SiH, Si and H species, depending on the stereo-chemical structure of excited states (*Matsuda 2004*). If H_2 carrier gas is introduced in the plasma, it can be decomposed into atomic H. The reactive species will experience secondary reaction mostly with the parent molecules of SiH_4 and H_2. This basically involves a lot of interactions as summarized in the literature (*Perrin et al. 1996*). The short lifetime species such as SiH_2, SiH and Si are highly reactive to the interactions. This results in the conversion into the long-lived species (SiH_3) or higher order silane species (Si_xH_y), while, long lifetime species of SiH_3 are

generally inert to the reaction with the parent molecules. In a steady state of silane plasma, SiH_3 species are dominant with number density of $10^{11} – 10^{13}$ cm^{-3} compared to the SiH_2, SiH and Si with number density < 10^{10} cm^{-3} (*Matsuda 2004*). Thus, SiH_3 is the main precursor corresponding to the growth. The high silane species, such as Si_2H_6 and Si_3H_8 could result in the cluster formation, which is usually prohibited from growth.

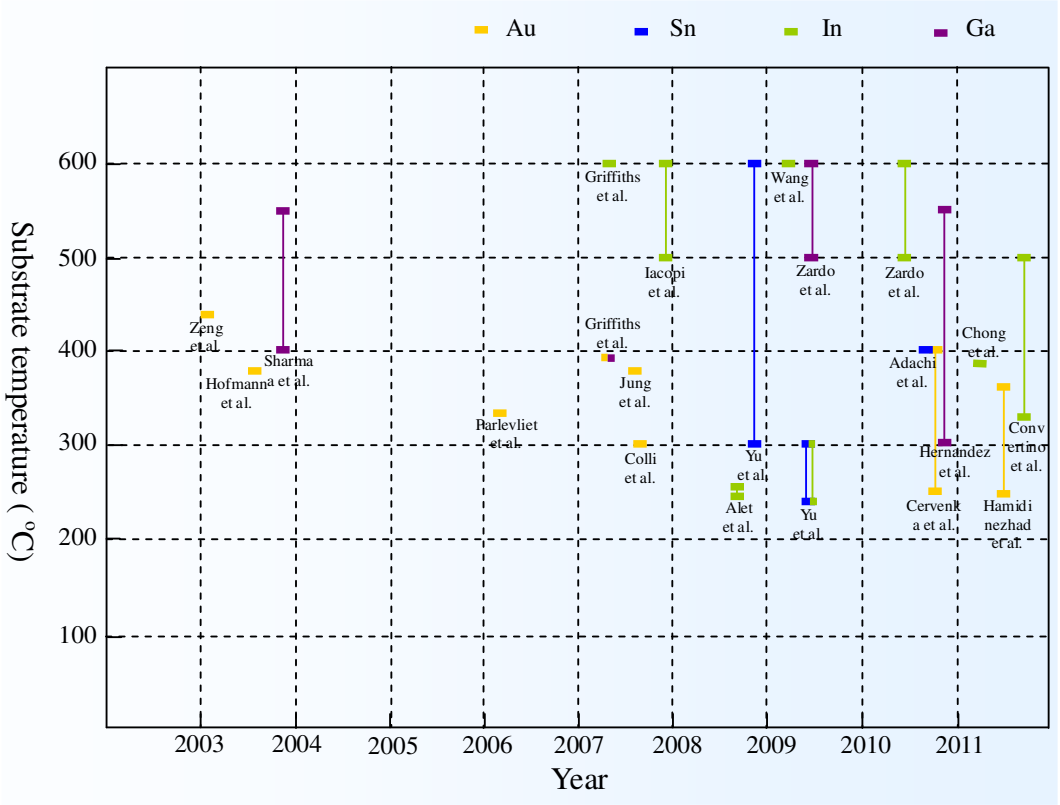

Figure 2.10: Summary of the reported works on the PECVD growth SiNWs from year 2003-2011. (*Adachi et al. 2010; Alet et al. 2008; Červenka et al. 2010; Cervera et al. 2010; Chong et al. 2011; Colli et al. 2007; Convertino et al. 2011; Griffiths et al. 2007; Hamidinezhad et al. 2011; Hofmann et al. 2003; Iacopi et al. 2007; Jung et al. 2007; Parlevliet and Cornish 2006; Sharma and Sunkara 2004; Wang and Li 2009; Yu et al. 2008; Yu et al. 2009; Zardo et al. 2009; Zardo et al. 2010; Zeng et al. 2003*)

The reported works on the synthesis of Au-catalyzed SiNWs using PECVD were initiated by Zeng et al. in early 2003 (*Zeng et al. 2003*). Hofmann et al. showed that the growth rate of the Au-catalyzed SiNWs grown by PECVD is ~1 order of magnitude higher than thermal CVD, while the growth is initiated at a low substrate temperature of 380°C (*Hofmann et al. 2003*). Plasma dissociation of SiH_4 induces high quantities of reactive SiH_x species, thus it allows the NWs grown from low Si solubility catalyst,

especially Sn, In and Ga. Such low Si solubility catalyst seems to be favoured in more recent studies due to their low melting temperature. The substrate temperature as low as 240^{o}C for the successful growth of SiNWs was achieved by using In and Sn as catalyst (*Yu et al. 2009*). Different from the CVD, selective growth and random growth rather than epitaxial growth of SiNWs are found using PECVD. This can be due to the random process in plasma. The NWs grown by PECVD usually reveal a tapering feature. This shows that the radial growth appears more significant in plasma. Moreover, excess ion bombardment by high energetic ion (especially for high rf power) is found to destroy the crystallinity of the NWs (*Hofmann et al. 2003*).

2.4.3 Hot-wire chemical vapour deposition

HWCVD is another option for low temperature CVD technique. Different from PECVD, it utilizes a metallic catalyzer to decompose SiH_4 precursor. HWCVD is constructed by metallic (usually tungsten or tantalum) filament coils, which serve as catalyzer. The filament coils are connected to a high voltage power source which supplies power to heat up the filament for deposition. The catalyzer can be designed and scaled up by increasing the surface area of the catalyzer for large area deposition. The figure of merit of the HWCVD is the ion free deposition. The absence of ion bombardment and surface charge effects can eliminate the surface and structural defects on the SiNWs. High dissociation rate of SiH_4 using HWCVD can thus enhance the deposition rate to ~1 order higher than PECVD (*Matsumura et al. 2004*). H atom density of HWCVD is about one to two orders higher than PECVD (*Masuda et al. 2002*). Since H atoms play a crucial role in the formation of crystalline Si structures, a sample prepared using HWCVD can easily form crystalline structures with less or without H_2 dilution (*Hiza et al. 2006; Jadkar et al. 2003*).

Tungsten filament is commonly used for SiH_4 decomposition with filament temperature, T_f in a range from 1500 to 2000°C (*Duan et al. 2001; Tonokura et al. 2002; Van Veenendaal and Schropp 2002; Zheng and Gallagher 2006*). SiH_4 molecules are dissociatively absorbed on the surface of tungsten filament in a form of Si and H at filament temperature, T_f > 1500°C. The Si- and H-bonded to tungsten are then catalytically cracked and desorbed into Si and H radicals following the process as (*Matsumura et al. 2004; Tonokura et al. 2002; Van Veenendaal and Schropp 2002*):

$$SiH_4(g) \rightarrow Si(g) + 4H(g) \quad (2.5)$$

At pressures higher than 5 μbar, the Si radicals can interact with SiH_4 parent molecules, resulting in the yield of $HSiSiH_3$ species (*Van Veenendaal and Schropp 2002*). As $HSiSiH_3$ is unstable, it will react with SiH_4 again to form more stable H_2SiSiH_2 radicals. The reactions can be simplified as:

$$Si(g) + SiH_4(g) \rightarrow Si_2H_4(g) \quad (2.6)$$

The presence of H radicals can result in the interactions with SiH_4 molecules as (*Nozaki et al. 2001*):

$$H(g) + SiH_4(g) \rightarrow SiH_3(g) + H_2(g) \quad (2.7)$$

The SiH_3 radical does not react with SiH_4 molecules due to its higher stability. Hence, the SiH_3 and Si_2H_4 radicals are generally two candidates corresponding to the growth.

The implementation of HWCVD in the growth of one-dimensional SiNWs was first tried by Hwang et al. (*Hwang et al. 2000*) using a tungsten filament heated at 1800°C. However, they showed that the NWs growth was completely suppressed and resulted in Si film deposition after introducing an HW into the reactor. The first successful VLS grown of needle-shaped Si wire arrays was achieved by Govindarajan et al. (*Govindarajan et al. 2009*). Nevertheless, the wires possess low aspect ratio (~3) and large diameter of several to tens of microns. On the other hand, Ma et al. (*Liu et al.*

2009) combined the glancing angle deposition and HWCVD techniques to prepare vertical aligned microcrystalline Si nanorod arrays. Similarly, Lefeuvre et al. (*Lefeuvre et al. 2011*) utilize porous anodic alumina template in HWCVD to produce well-organized vertical SiNWs. More recent work reported by Meshram et al. (*Meshram et al. 2011*) demonstrated the growth of SiNWs using HWCVD and Au catalyst without assistance of other techniques. As they mentioned, the recipe for successful growth is much related to the H_2 pre-treatment process to produce nanosized metal islands prior to the growth. Nevertheless it should be noted that their SiNWs are amorphous in structure.

2.5 NOVEL STRUCTURES OF SILICON NANOWIRES AND THEIR GROWTH MECHANISMS

SiNWs synthesized by different techniques reveal different morphology and structural properties. They can be present in rod-, tip-, needle-, cone-, chain-, spiral- and coil-shaped structures (*Ramanujam et al. 2011*). Their structural properties can vary from monocrystalline, poly, micro, to nano, polymorphous, or mixed phase structures (*Rurali 2010*). Different morphologies and structures of SiNWs can be suited to different kinds of applications in nanotechnology.

In this section, the successful growth of several novel Si structures including chain-like SiNWs, SiC capped Si nanotips and homogenous core-shell SiNWs by using thermal evaporation, ECR plasma etching, and PECVD, respectively, are described. The structural properties as well as the growth mechanisms of the respective structures are also discussed.

2.5.1 Chain-like Si nanowires

Chain-like SiNWs were first grown by Lee's group using a mix of Si and SiO_2 powder via thermal evaporation (*Wang et al. 1998*). Figure 2.11 (a) shows a TEM micrograph of the SiNWs prepared from pure Si powder mixed with ~70 wt% of SiO_2, heated at temperature of 1200^{o}C for 12 hours. Two kinds of morphologies, namely uniform diameter SiNWs and chain-like SiNWs were formed through the evaporation. The HRTEM micrograph of the chain-like SiNWs is shown in Figure 2.11 (b). The chain-like NW is constructed by the linkage of Si nanocrystallites. Si nanocrystallites with size of several to tens nm are linked by amorphous SiO_2 to form chain structures.

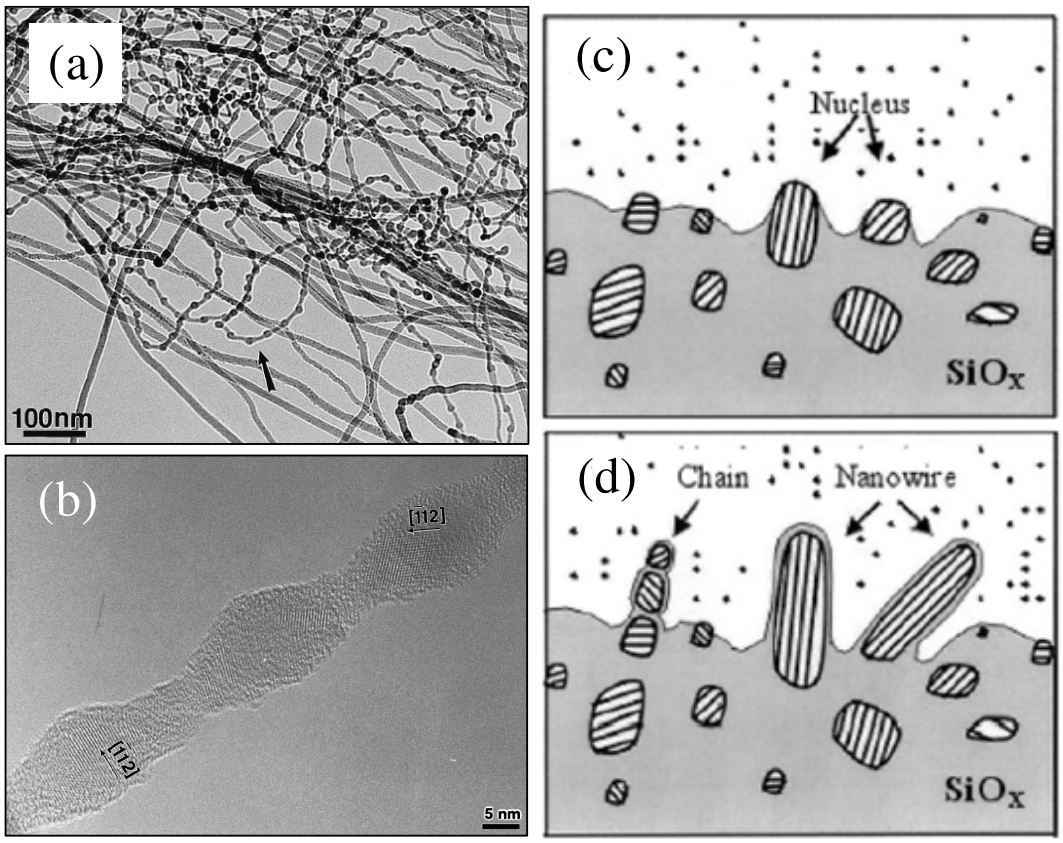

Figure 2.11: (a) TEM image of the SiNWs synthesized using thermal evaporation of SiO_x powder. (b) HRTEM image of chain-like SiNWs (*Wang et al. 1998*). Schematic of the (c) nucleation and (d) growth mechanism of the chain-like SiNWs. The parallel lines indicate [112] orientation (*Lee et al. 1999*).

Lee et al. proposed that the growth of the chain-like SiNWs is assisted by Si oxide and

named it oxide-assisted growth (*Wang et al. 1998*). The schematic of the growth mechanism is presented in Figures 2.11 (c) and (d). SiO_2 vapour is deposited first and forms a SiO_x matrix. Si nanocrystallites are formed by reduction of Si_xO vapour. The Si nanocrystallites are covered by shells of SiO_x which act as nuclei to catalyze the growth of NWs. The nuclei with a preferred orientation will grow at a high rate to form uniform diameter SiNWs, while nuclei with non-preferred orientation may form chain-like SiNWs. The chain-like NWs showed much higher PL intensity than the uniform diameter NWs (*Sun et al. 2004*).

2.5.2 SiC capped Si nanotips

Vertical aligned Si nanotip arrays were successfully fabricated by Chen's group using self-masked dry etching technique via an ECR plasma CVD reactor (*Hsu et al. 2004*). The fabrication process was carried out in plasma of a mixture of argon (Ar), methane (CH_4), H_2 and SiH_4 gases on a plain Si substrate. Figure 2.12 (a) shows a typical SEM cross-section image of the Si nanotip arrays obtained after one hour deposition. The technique has proved compatible for wafer scale of Si nanotip arrays fabrication. The HRTEM micrograph [Figure 2.12 (b)] shows that the top of Si nanotip is covered by a SiC cap. An ultra-fine tip with apex radius of ~1 nm is achieved by this SiC capped Si nanotips. Meanwhile, high electron field emission with turn on field of < 1 V/μm at current density of 10 $\mu A/cm^2$ is demonstrated by the Si nanotip arrays (*Lo et al. 2003*). Schematic diagram of the growth model of the Si nanotip is illustrated in Figure 2.12 (c). The Ar, CH_4, H_2 and SiH_4 gases are decomposed within the ECR plasma region. SiH_4 and CH_4 plasmas will tend to form SiC clusters which uniformly distributed on the surface of the substrate. While, the Ar and H_2 plasmas are responsible for the physical and chemical etching, respectively, of the Si substrate. The SiC clusters act as a mask against the etching process. The Si layer is etched at a much faster rate than the SiC

layer, thereby resulting in the formation of SiC capped Si nanotips.

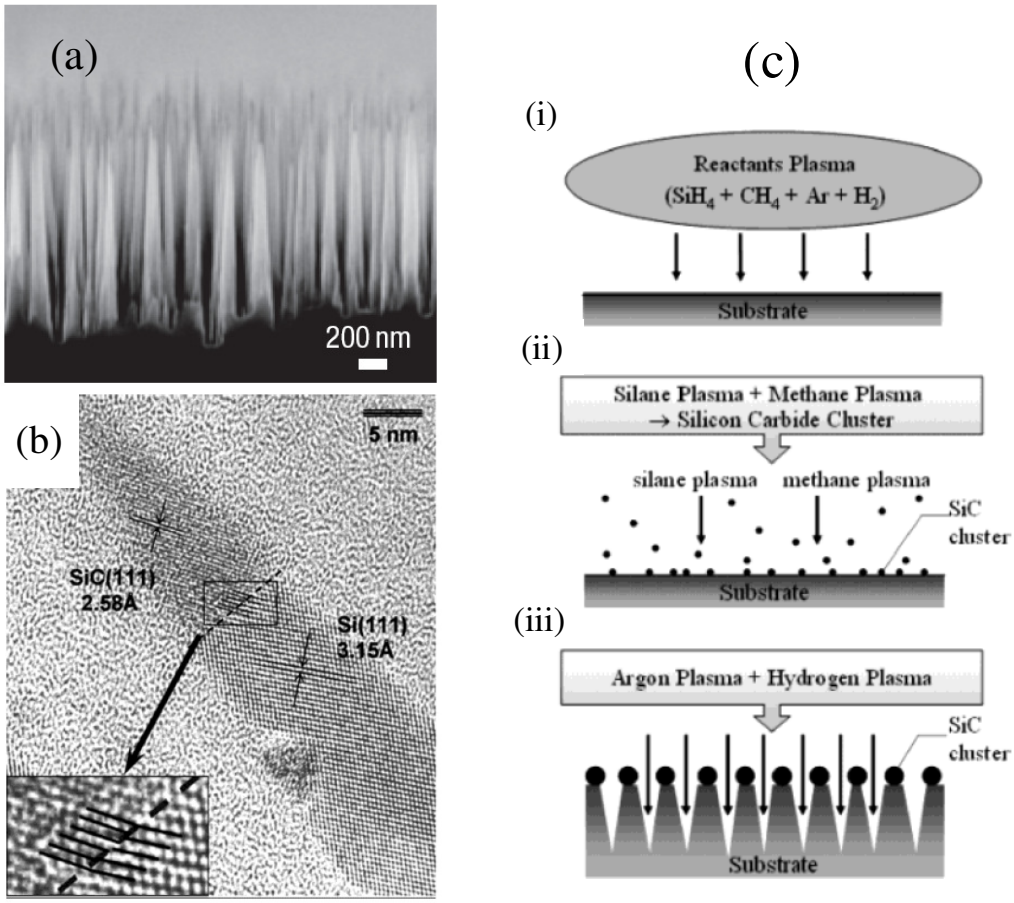

Figure 2.12: (a) Cross-sectional SEM image of Si nanotip arrays fabricated by a dry etching method using ECR plasma (*Huang et al. 2007*). (b) HRTEM image of a Si nanotip (*Lo et al. 2003*). (c) Schematic diagram of the formation of Si nanotips (*Hsu et al. 2004*).

2.5.3 Crystalline-amorphous core-shell Si nanowires

Crystalline Si core and amorphous Si shell NWs are demonstrated by Karim's group using Sn catalyst and PECVD technique (*Adachi et al. 2010*). The SEM image of the Sn-catalyzed SiNWs is shown in Figure 2.13 (a). TEM and HRTEM micrographs reveal the crystalline NWs core and the amorphous Si layer surrounding the core. They noticed that the thickness of the amorphous Si layer is constantly increased from 60 to 100 nm when the rf power density increased from 13.7 to 19.5 mW/cm^2, thereby proving that the thickness of the amorphous Si layer can be controlled by controlling the rf power density. A growth model of SiNWs from low solubility metal and PECVD technique is

illustrated in Figure 2.13 (d). In SiH_4 and H_2 plasma, H radicals can act to reduce the outer oxide layer of the molten Sn catalyst droplets, while, pre-cracked SiH_x radicals in plasma totally crack into Si atoms on the surface of the molten Sn droplets and diffuse into it. The Si atoms then form precipitation at the liquid-solid interface and produce axial growth of crystalline SiNWs. During the growth process, the uncatalyzed reactive SiH_x, especially SiH_3 radicals form deposition of amorphous Si structures on the walls of the NWs. This results in the crystalline-amorphous core-shell SiNWs formation.

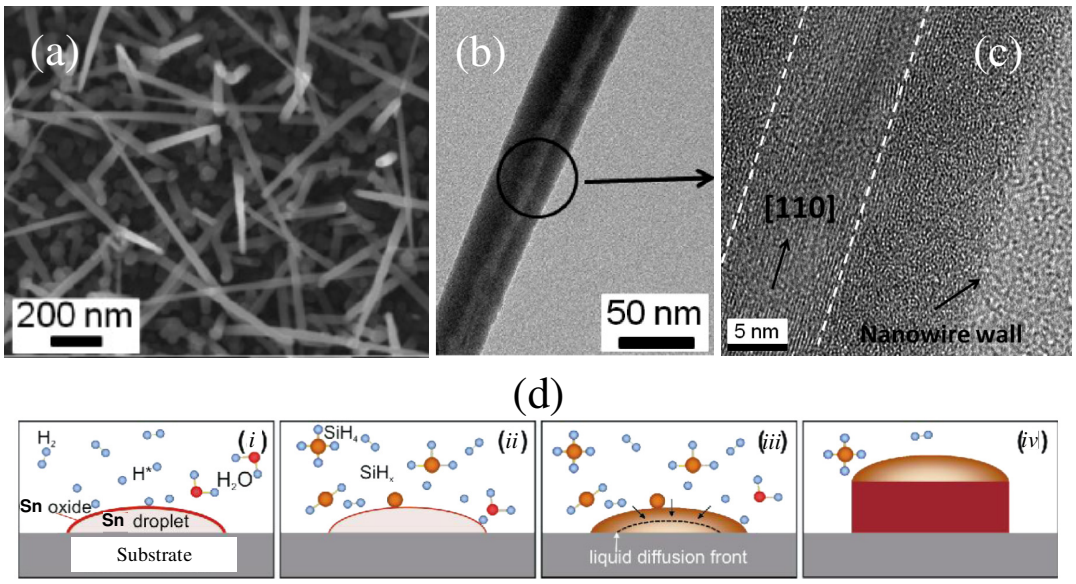

Figure 2.13: (a) SEM image of Sn-catalyzed SiNWs grown using PECVD. (b) TEM, and (c) HRTEM micrographs of a crystalline core and amorphous shell SiNW (*Adachi et al. 2010*). (d) Schematic of the VLS growth mechanism of the SiNWs in the presence of plasma (*Zardo et al. 2009*).